Wear 274–275 (2012) 355–367

Contents lists available at SciVerse ScienceDirect

Wear

journal homepage: www.elsevier.com/locate/wear

# Wear at the die radius in sheet metal stamping

Michael P. Pereira[a,*], Wenyi Yan[b], Bernard F. Rolfe[c]

[a] Centre for Material & Fibre Innovation, Deakin University, Geelong, VIC 3217, Australia
[b] Department of Mechanical & Aerospace Engineering, Monash University, Clayton, VIC 3800, Australia
[c] School of Engineering, Deakin University, Geelong, VIC 3217, Australia

ARTICLE INFO

*Article history:*
Received 3 August 2010
Received in revised form 9 October 2011
Accepted 13 October 2011
Available online 20 October 2011

*Keywords:*
Contact pressure
Failure
Galling
Sheet metal stamping
Tool wear

ABSTRACT

In sheet metal stamping, it is known that wear is unevenly distributed over the die radius and that multiple wear mechanisms may occur simultaneously. However, there has been little or no work that details the types of wear mechanisms, and quantifies the locations at which they occur. Furthermore, the link between recently identified time-dependent contact conditions and the wear response is currently unknown. An experimental study is presented in this paper to examine the location, type and severity of wear that occurs over the die radius during a typical sheet metal stamping process. It is found that the wear over the die radius consists of a combination of ploughing and galling mechanisms. The relative severity of the ploughing mechanism is divided into two distinct zones on the die radius, which correlate well with the contact pressure and sliding distance behavior predicted in our recently published numerical study. The galling mechanism results in failure of the stamping process and is, therefore, critical to the overall tool wear response. Our analysis indicates that the severe contact pressure/small sliding distance conditions, which occur during the initial stage of the process, cause the galling behavior observed over the radius. Therefore, it is concluded that the overall tool wear response and tool life is primarily dependent on the initial transient stage of the stamping process.



## 1. Introduction

In the automotive sheet metal stamping industry, an understanding of tool wear has become increasingly important due to the implementation of higher strength sheet steels and the reduced use of lubricants in the press shop. Tool wear has often been examined through the use of 'representative' wear tests, such as simple two-body sliding contact situations [1–3] or bending-under-tension-type operations [4–9]. These processes result in steady contact conditions at the wearing interface, which are assumed to represent the important wear conditions experienced during sheet metal stamping. However, several studies have shown that non-steady contact conditions exist at the die radius in sheet metal stamping [9–15]. Although a large portion of the stamping process exhibits steady contact conditions that qualitatively compare well with bending-under-tension processes, it has recently been identified that there is a distinct initial transient stage that exhibits severe and time-dependent contact conditions [13–15] (see Fig. 1). As shown in Fig. 1a, the contact pressures that occur at the die radius during the transient stage are well in excess of those experienced during the steady-state stage. Furthermore, it has been shown that the transient stage results in unique contact pressure [13], sliding distance [14], and bulk deformation conditions [15] at the wearing interface, which differ significantly to those experienced during traditional wear tests. It has been speculated by Pereira et al. [13–15] that the contact and deformation conditions that exist during the transient stage may be critical to the overall sheet metal stamping tool wear response.

It is well known that several different wear mechanisms – including micro-cutting, ploughing, ratchetting and galling – can occur during sheet metal stamping. The literature reveals that the location of wear on the die radius, the type of mechanism that occurs, and the relative severity of the wear response can vary significantly (for example, see [2,16–18]). This variation can often be observed at different locations over a single die radius surface for a given stamping process. For bending-under-tension processes, the location, type and severity of wear shows close correlation to the characteristic two-peak contact pressure distribution that exists over the tool radius [4,6,8,19,20]. However, for sheet metal stamping processes, the correlation between the wear behavior and the contact conditions is currently unknown.

Through the use of surface profilometry, the wear depth over the die radius has been characterized for the case of a cylindrical cup forming process [16,21]. This method can successfully quantify wear mechanisms that involve material removal, such as the micro-cutting wear mechanism. However, when material is not removed from the surface – i.e. when ploughing, galling, or a

* Corresponding author. Tel.: +61 3 5227 3353; fax: +61 3 5227 1103.
*E-mail addresses:* michael.pereira@deakin.edu.au (M.P. Pereira), wenyi.yan@monash.edu (W. Yan), bernard.rolfe@deakin.edu.au (B.F. Rolfe).

0043-1648/$ – see front matter © 2011 Elsevier B.V. All rights reserved.
doi:10.1016/j.wear.2011.10.006

combination of abrasive and adhesive mechanisms occurs together – the surface profilometry/wear depth results can be more difficult to interpret. In these cases, microscopy or visual observation has been used to identify the predominant wear mechanisms [17,18]. However, to the authors' knowledge, there is no published work that details the types of wear mechanism, and quantifies the locations at which they occur, over the die radius in sheet metal stamping. This knowledge is especially important, considering the varying contact conditions that have been identified to occur, both over the die radius and throughout the duration of the stamping process. Therefore, the first aim of this investigation is to characterize the location, type and severity of wear that occurs over the die radius, for a typical sheet metal stamping process.

Once the wear response has been characterized, the importance of the macro-scale contact, sliding and deformation conditions over the die radius can be examined. In particular, the conditions at the die radius that are critical to the overall tool wear behavior can then be determined. Therefore, the second aim of this investigation is to assess whether the recently identified transient stage of the stamping process, and the resulting transient conditions at the die radius (shown in Fig. 1a), are important to the overall wear response.

## 2. Experimental setup

### 2.1. Test method and configuration

The channel forming test shown in Fig. 2 forms the basis of this study. The test configuration, summarized in Table 1, is based on semi-industrial wear tests previously reported in the literature [17,22,23] and numerical studies conducted by Pereira et al. [13,14]. The geometric, process and material parameters closely represents a typical wear prone automotive sheet metal stamping operation. An Erichsen Universal Sheet Metal Testing Machine (Model 145-60) was used as the press system. The custom tooling (shown in Fig. 2) was designed to be compatible with the standard tooling available, while permitting easy removal of the die radius inserts for inspection and interchange.

**Table 1**
Summary of the geometric and process parameters for the channel forming operation.

| | | |
|---|---|---|
| Punch width | $a$ | 40 mm |
| Draw depth | $d$ | 50 mm |
| Initial holder force | $F_h$ | 20 kN |
| Die-to-punch gap | $g$ | 2.1 mm |
| Blank length | $l$ | 150 mm |
| Die corner radius | $R_d$ | 5 mm |
| Punch corner radius | $R_p$ | 5 mm |
| Blank thickness | $t$ | 2 mm |
| Blank width | $w$ | 19.5 mm |
| Punch speed | $v$ | 1.5 mm/s |

It is worth noting that there is a difference between the width of the punch, $a$, used in this study (40 mm), compared to that of the numerical studies (30 mm) [13,14]. However, comparison to the previous numerical study is still valid, as numerical analysis showed that this difference in punch width has negligible effects on the contact and deformation conditions at the die radius [13]. Additionally, the punch speed, $v$, of 1.5 mm/s is significantly slower than the ram speeds used in typical automotive sheet metal stamping processes [23]. The authors appreciate that the effects of deformational and frictional heating, at higher punch speeds, may influence the tool wear rate and mechanisms produced. However, investigation of these effects is beyond the scope of this work and is not considered in this study.

As previously stated, one of the primary aims of the tests was to determine the wear behavior that was critical to the overall tool wear response – i.e. the type of wear mechanism and the location

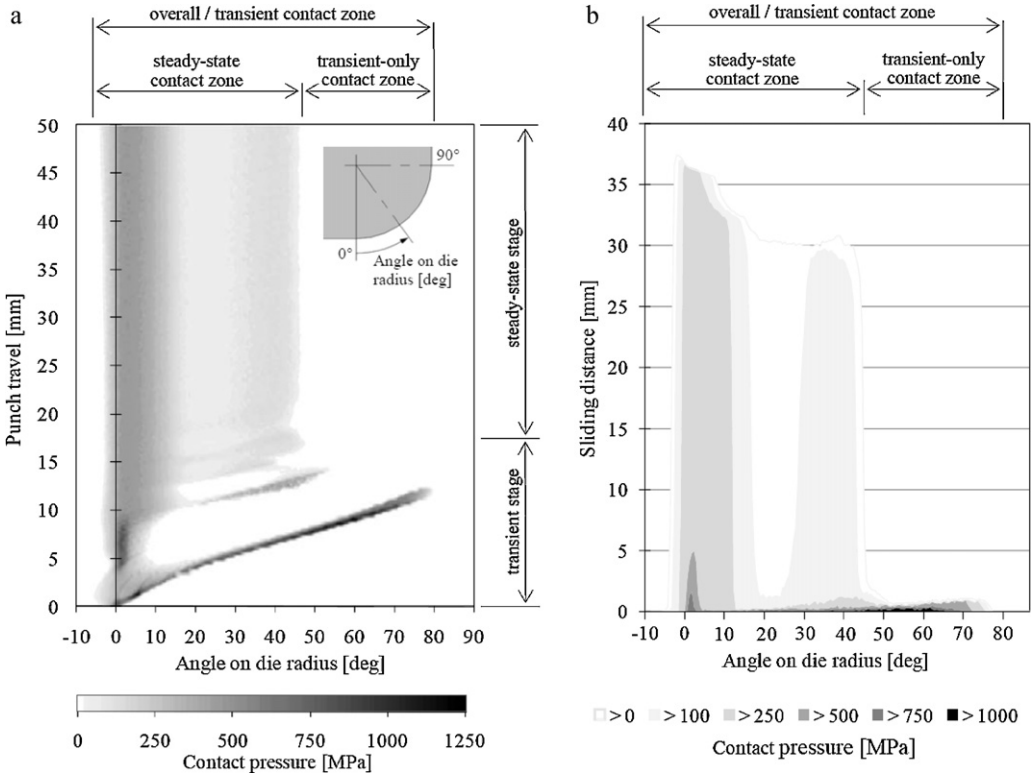


**Fig. 1.** Discontinuous and time-dependent contact conditions experienced over the die radius during a typical sheet metal stamping operation. (a) Evolution of contact pressure, showing the existence of two distinct stages (adapted from [13]). (b) Sliding distance distribution experienced over die surface at different magnitudes of contact pressure (adapted from [14]).

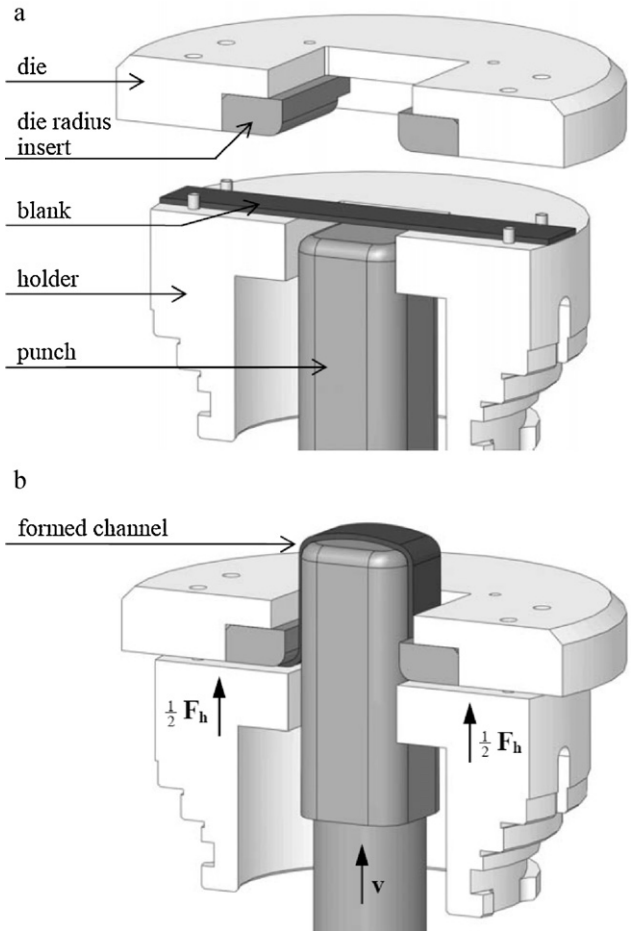


**Fig. 2.** Channel forming wear test and tooling, using an Erichsen Universal Sheet Metal Testing Machine: (a) prior to, and (b) at the end of the stamping process.

on the die radius that results in failure of the stamping process. For automotive sheet metal stampings, failure is typically judged by the existence of visible scratches on the sidewalls of the formed parts [17,22]. Therefore, after each forming operation, the sidewalls of the stamped parts were carefully visually inspected for any signs of wear. It is known that the wear rate (for galling, in particular) can increase very rapidly once the process has initiated [18,24]. Therefore, to obtain accurate information on the type and location of wear, it was important to stop the testing process as soon as the initiation of the critical wear mechanisms was evident. For this reason, the surfaces of the die radius inserts were also closely visually examined after each part was stamped.

It is appreciated that a combination of visual inspection and surface profilometry (i.e. the measurement of scratch depths) on the stamped part sidewalls can be used to provide an indication of the wear state of the process [17]. However, in this investigation, the authors found that visual inspection alone provided an efficient and successful method of identifying the development of the critical wear response. This was especially the case because of the need and desire to stop the tests when the critical wear mechanisms were first visible. Once the test was stopped, the die radius insert surfaces were cleaned with acetone and examined in detail with surface profilometry and optical microscopy techniques (as will be described in Section 2.3).

Prior to the tests, the edges of the sheet metal blank were deburred to remove any sharp edges associated with the guillotine operation that was used to cut the blanks to size. All tools and blank surfaces were wiped with acetone using a lint-free cloth before each

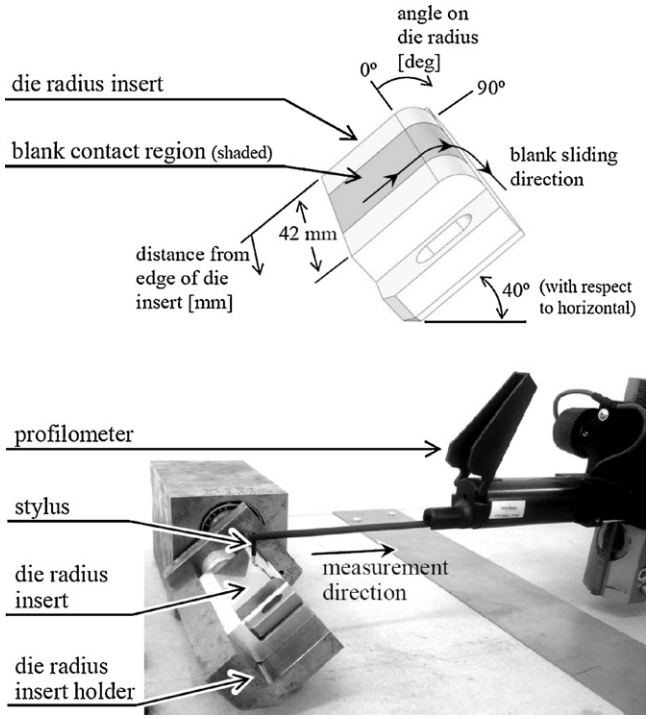


**Fig. 3.** Surface profile measurements along the blank sliding direction.

sample was formed. Sufficient time was allowed to ensure that the acetone had evaporated from the active surfaces prior to each test. Lubrication was not used.

### 2.2. Materials

The tools that contacted the blank during the forming stroke (die, die radius inserts and blank holder) were manufactured from AISI D2 tool steel and through-hardened to 60 HRC. D2 grade tool steel was chosen as it is commonly used in the automotive industry for stamping press tooling [17]. The blank material was an uncoated dual phase (DP600) sheet steel, with a strain hardening index of 0.15, yield strength of 400 MPa and tensile strength 660 MPa, as determined from tensile tests.

### 2.3. Surface characterization

A combination of surface profilometry and optical microscopy was used to characterize the surface of the die radius inserts prior to and after the stamping wear tests. The form (shape) of the die radii were measured using 2D profilometry along the blank sliding direction, while the roughness was measured in both the sliding and transverse directions.

#### 2.3.1. Surface profile (form) measurements along the sheet sliding direction

The surface profilometry was conducted using a Taylor Hobson Form Talysurf Intra (112/3477–01) instrument with a custom, 120 mm long, 60 degree conical, 2 μm radius, diamond tipped stylus. The stylus sliding speed and sampling rate were 1 mm/s and 2000 Hz, respectively.

Each die insert was positioned at an angle of 40 degrees to the horizontal, while the form of the die radius surface was measured along the blank sliding direction using a single horizontal traverse of the stylus, as shown in Fig. 3. The region of approximately −5 to 80 degrees on the die radius was measured using a 7 mm measurement length. This measurement was repeated at three locations

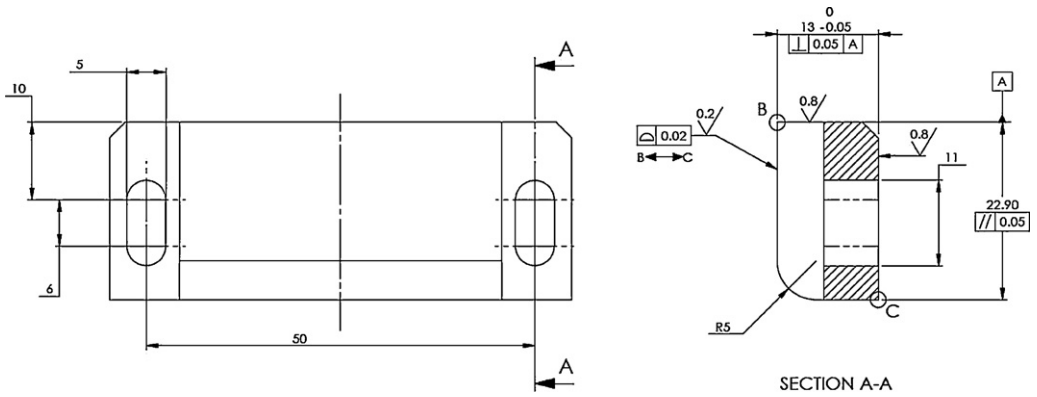


**Fig. 4.** Excerpt from the engineering drawing of the die radius insert. All dimensions in mm. General linear tolerance ±0.2 mm.

across the die radius – i.e. at distances of 15, 20 and 25 mm, as measured from the edge shown in Fig. 3. Note that the blank material contacts the die radius insert surface at the region of approximately 11–31 mm from the die radius insert edge, as indicated by the shaded region on the die radius insert in Fig. 3.

Careful attention was given to the manufacture and measurement of the die radius inserts in this study. It was rationalized that the shape of the die radius surface should be manufactured precisely – particularly regarding the cylindricity of the radius surface, and the accuracy of the transition between the radius and the flat surfaces. Therefore, a small profile tolerance of ±0.02 mm was specified on the active surfaces of the die radius insert (refer to surface B–C shown in Fig. 4). However, the tolerance on the size of the die radius was set to ±0.2 mm in order to minimize costs.

The quality of each die radius was checked by calculating the deviation of the measured profiles with respect to an ideal profile shape. The ideal profile consisted of a horizontal line with a perfectly round radius exactly tangent to the horizontal line. The error between one of the measured profiles and an ideal profile is shown in Fig. 5, as calculated using a mathematical solver routine developed in Microsoft Excel. The horizontal line of the *x*-axis can be considered as the ideal profile, while the curve shows the deviation of the measured profile from this ideal. The solver minimized the error between the measured and ideal profiles, through translation and rotation of the measured profile in two-dimensional space. As part of the error minimization routine, the radius of the ideal profile was also permitted to vary within ±0.2 mm, in accordance with the manufacturing tolerance specified. For the measured die radius profile examined in Fig. 5, the best fit to the ideal profile was achieved with a radius of 5.048 mm.

It is evident that the die surface profile shown in Fig. 5 is very accurate, with a maximum variation from ideal of less than 0.004 mm for the entire region from approximately −5 to 80 degrees on the die surface. For each of the three measurements taken across each of the die radius surfaces tested, the maximum profile deviation was calculated to be less than ±0.006 mm for the region between −5 and 75 degrees on the die surface. Note that this region (from −5 to 75 degrees) approximately corresponds to the predicted blank contact zone, as shown in Fig. 1. Hence, any effects associated with manufacturing inaccuracies are assumed to have a negligible effect on the wear results obtained in this study.

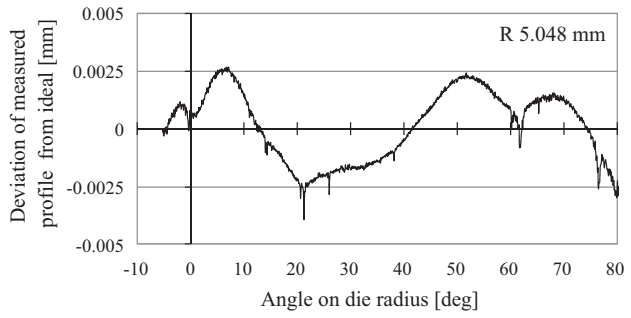


**Fig. 5.** Deviation of a measured profile (die radius insert II at 20 mm from edge) with respect to an ideal profile shape. The ideal radius was taken as 5.048 mm for the case shown.

### 2.3.2. *Surface roughness measurements along the sliding and transverse directions*

The profile measurements, described above, were used to calculate the roughness of the die radius inserts in the sliding direction. For the transverse direction, the die insert holder device was used to position the die insert at the angle $\theta$ from the horizontal, such that the stylus was positioned at the same angle $\theta$ on the die radius surface (see Fig. 6). As shown, the transverse direction roughness measurements were taken from 15 to 27 mm from the die insert edge. The measurement was repeated at 10 degree increments on the die radius, from 0 to 80 degrees. For each profile measurement,

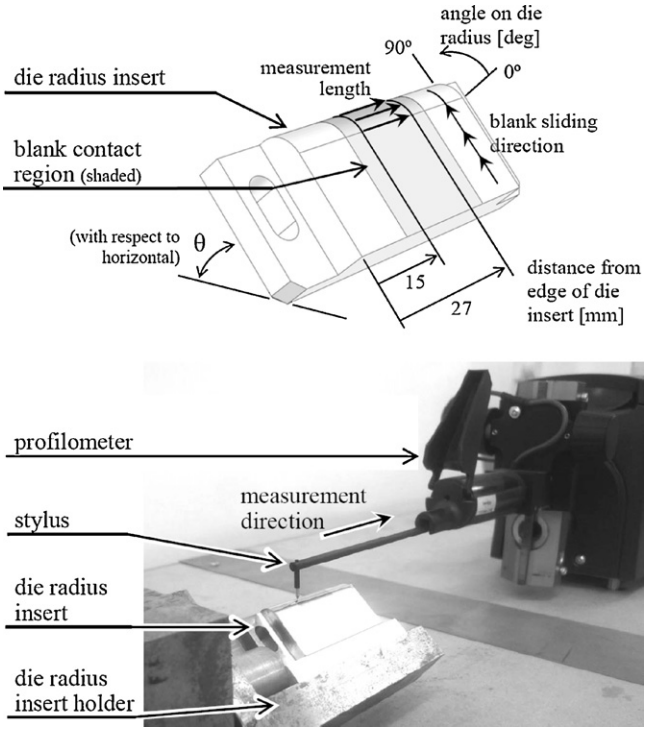


**Fig. 6.** Surface profile measurements transverse to the blank sliding direction.

**Table 2**
Parameters used for the roughness analysis.

| | |
|---|---|
| Upper cut-off, $l_c$ | 0.25 mm |
| Short wavelength cut-off, $l_s$ | 2.5 μm |
| Evaluation length, $l_n$ | |
| Sliding direction | 7 mm |
| Transverse direction | 12 mm |
| Bandwidth | 100:1 |
| Filter | Gaussian |

the Taylor Hobson Ultra software (version 5.5.4.20) was used to calculate the mean arithmetic roughness, *Ra*, using the parameters detailed in Table 2.

For typical *Ra* calculations, the upper cut-off length ($l_c$, shown in Table 2) is used to suppress irregularities that occur over longer lengths, such that the surface roughness can be determined [25]. Therefore, in the same way that the surface roughness is calculated for a nominally flat surface with some waviness, the Gaussian filter and filter cut-off was used to separate the roughness from the nominal form associated with the curved surface of the die radius inserts. To choose the most appropriate filter cut-off for the correct calculation of *Ra*, a pragmatic empirical approach was utilised, based on the procedure detailed in [25]. Using this approach, a Gaussian roughness filter was applied, starting with the longest cut-off available (8 mm) and finishing with the shortest cut-off available (0.08 mm), and the resulting 'modified' surface profile was observed in each case. Considering all the profile measurements in the sliding direction, the upper cut-off length of 0.25 mm gave the best compromise between highlighting the surface features of interest (i.e. the roughness), while suppressing the form to a minimal amount. Utilising this empirical approach, it was clear that the smaller cut-off length of 0.08 mm suppressed the roughness itself, while the larger cut-off of 0.8 mm did not eradicate the form sufficiently – hence these were not suitable for the roughness calculations. It should be noted that the value of upper cut-off length chosen (0.25 mm) also closely corresponds to the cut-off recommended by the relevant ISO standard [26], for the values of *Ra* measured in the study.

### 2.3.3. Optical microscope imaging

The die radius inserts were positioned on the optical microscope stage at angles of 0–80 degrees from the horizontal; in 10 degree increments (see Fig. 7). At each angle, a series of digital photographs were captured through the 10× optical lens at 1 mm increments along the transverse direction. Using this method, the region of the surface from 0 to 80 degrees on the radius and 14–28 mm from the die insert edge was examined. A full set of micrographs was captured at the end of the test, corresponding to approximately 120 images for each of the die radius insert surfaces, in order to obtain a detailed understanding of the wear behavior. This was a very time-consuming task; therefore, fewer micrographs were taken prior to the tests. The aim, in this case, was to obtain a general understanding of the initial surface topography, in combination with the roughness measurements described in Section 2.3.2.

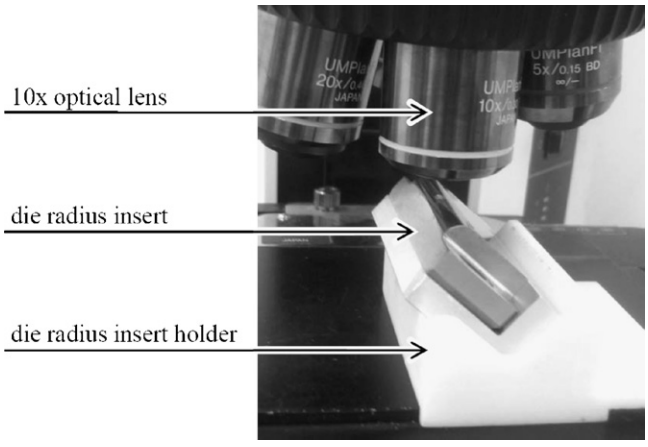


**Fig. 7.** Optical microscope setup for imaging of the die radius insert surfaces. The die insert is positioned at an angle of 40 degrees to the horizontal for the case shown.

### 2.4. Test conditions

The details of the individual channel forming wear tests examined in this study are summarized in Table 3. These are in addition to the general geometric and process parameters specified in Table 1. The values of the die radius, maximum profile deviation and roughness are average values obtained from the surface profilometry measurements and calculations described in Section 2.3. As shown in Table 3, the primary differences between each of the tests were the specified drawing depth and the method used to prepare the die radius insert surfaces.

With regards to the surface preparation method employed; die radius inserts I, V and VI were polished by hand, using 1200 grit silicon carbide wet and dry sandpaper on a flat sheet of glass. Die radius insert II was also polished by hand, using the same method, but with 2400 grit sandpaper. Die radius insert III was polished using a cotton polishing wheel that was attached to a bench grinder, with small amounts of metal polishing compound. In each of these cases, the active surfaces (surfaces B–C shown in Fig. 4) were polished along the transverse direction after the final machining process. Die radius insert IV was not polished, with the active surfaces utilised in the as-machined condition.

Fig. 8 shows a complete view of the initial die radius surfaces, along the middle of the blank contact region. To construct these images, a single 'line' of the optical micrographs along the sliding direction was manually 'stitched' together. The method used to capture the individual images and construct the image sets ensured that the precise location of the micrographs along and across the die radius surface was established, as shown by the axes in Fig. 8. This knowledge was crucial for the examination of the worn die radius surfaces, as will be detailed in Section 3.

Fig. 8 provides a concise visual summary of the initial surface topography of the die radius insert surfaces. Examination of die insert IV shows that a significant amount of grinding marks, from the manufacturing process, are present on the die radius surface in the as-machined condition. This is further evidenced by the measured *Ra* values of 0.38 μm and 0.12 μm in the sliding and transverse directions, respectively (see Table 3). The hand polishing method, using the 1200 grit wet and dry sandpaper (refer to dies I, V, VI), removed most of these manufacturing grinding marks. For these cases, the surface topography is characterized by numerous light scratches along the transverse direction and reduced *Ra* values in both the sliding and transverse directions. Finally, it is evident that both the hand polishing method with the 2400 grit sandpaper and the machine polishing method (dies II and III, respectively), did not completely remove the grinding marks. However, the deeper grinding 'grooves' that were still present on the die surface (i.e. the vertical or near vertical lines observed on dies inserts II and III in Fig. 8b and c), did not appear to have a marked effect on the measured *Ra* values.

With regards to the drawing depths used; the value of 50 mm, used for Tests I–IV, represents the full drawing depth of the representative channel forming process previously examined experimentally [22,23] and numerically [13,14]. The drawing depth of 17 mm, used for Tests V and VI, was chosen to capture only the transient stage of the forming process, which was identified to occur from 0 to 17 mm of punch travel (see Fig. 1a).

**Table 3**
Details of the channel forming wear tests.

| Test/die radius insert label | I | II | III | IV | V | VI |
|---|---|---|---|---|---|---|
| Drawing depth (mm) | 50 | 50 | 50 | 50 | 17 | 17 |
| Die radius (*) (mm) | 5.080 | 5.051 | 5.047 | 5.062 | 4.998 | 5.036 |
| Maximum profile shape deviation (*) (mm) | 0.005 | 0.004 | 0.006 | 0.005 | 0.006 | 0.004 |
| Die radius roughness | | | | | | |
| Sliding direction (*) (μm) | 0.096 | 0.108 | 0.164 | 0.381 | 0.099 | 0.162 |
| Transverse direction (*) (μm) | 0.038 | 0.050 | 0.066 | 0.125 | 0.041 | 0.066 |
| Die radius surface preparation | Hand polished 1200 grit | Hand polished 2400 grit | Machine polished | As-machined | Hand polished 1200 grit | Hand polished 1200 grit |
| Total number of parts stamped | 30 | 14 | 14 | 18 | 10 | 25 |

*Note*: Items marked with an asterisk (*) denote average values measured using surface profilometry.

## 3. Results and discussion

The full stroke tests (Tests I–IV) were conducted to characterize the overall wear behavior over the die radius (see Section 3.1). Based on these findings, the short stroke tests (Tests V and VI) were conducted to assess the significance of the transient contact conditions on the overall wear response (see Section 3.2). The wear behavior at the die radius for each of the tests will be compared to each other and with respect to the contact and sliding conditions previously reported by the authors [13–15].

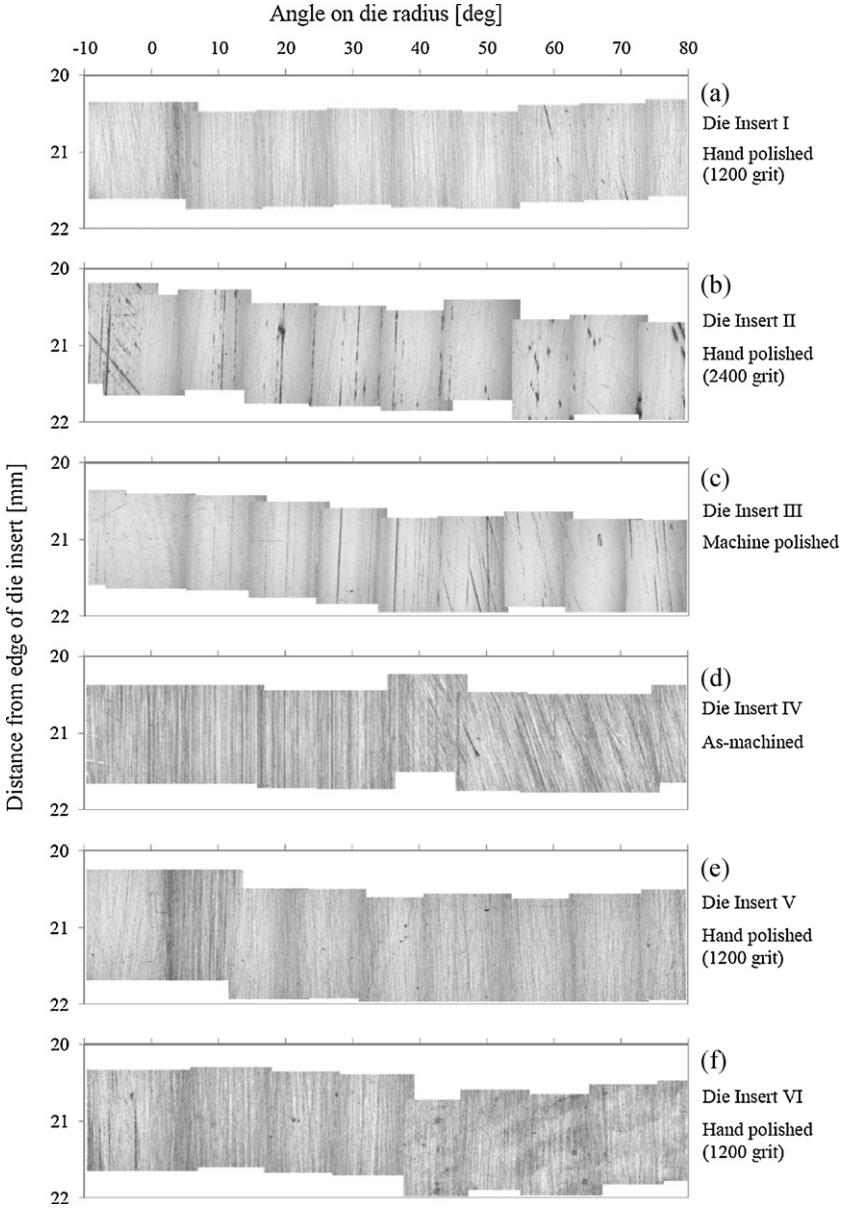


**Fig. 8.** Surfaces of the die radius inserts prior to the stamping wear tests. The blank sliding direction is from left to right.

### 3.1. Overall tool wear response (Tests I–IV)

The die radius insert surfaces were examined, using the surface characterization techniques described in Section 2.3, before the tests, at intervals of 15 stamped parts and at the end of the tests (when failure occurred). As previously stated, failure was defined to occur when scratches were first visible on the sidewall of the stamped parts, or at the first signs of galling on the die radius surfaces. The total number of parts to failure for each test is shown in Table 3, while Fig. 9 shows the sidewall of the last stamped part for each test. The severity of the scratches on the part surfaces was very slight in each case. However, through the use of careful lighting and flash photography, the scratches on the sidewalls of the parts are clearly visible in Fig. 9. Since this study aimed to examine the locations on the die radius that were critical to the wear response, it was important to capture these initial stages of wear, prior to the transition to more severe mechanisms due to the accumulated surface damage.

The optical microscope images were manually 'stitched' together to obtain a complete view of the cylindrical die radii surfaces, at key regions of interest. To highlight the general wear behavior, Fig. 10 shows the surfaces of die inserts I–IV at locations and/or instances where severe wear has not yet occurred. Die inserts I and IV were deemed to have failed when 30 and 18 parts were stamped, respectively. Therefore, Fig. 10a and d, which show the die surfaces after 15 parts were stamped, provide information about the general wear behavior prior to failure. Die inserts II and III failed at 14 parts. However, at this instant, scratches were not evident over the entire sidewall region of the stamped parts (see Fig. 9b and c). Therefore, to illustrate the wear behavior prior to failure, the regions on the dies shown in Fig. 10b and c correspond to locations on the sidewalls where scratches were not evident.

Fig. 11 shows the surfaces of die inserts I–IV at the end of the tests, at locations where severe wear is evident – i.e. at regions that correspond to the locations of scratches on the sidewalls of the stamped channels. The purpose of this figure is to highlight the wear behavior and locations on the die radius that are critical to the overall tool wear response.

#### 3.1.1. General observations

Figs. 10 and 11 provide a large amount of information relating to the wear and contact behavior over the die radius. Before discussing the specific response, it is worth highlighting a few general points regarding the stitched micrographs shown. Firstly, any non-horizontal markings on the die radii are likely to be manufacturing grinding marks or defects, which were present on the surfaces prior to beginning of the tests (see Fig. 8).

Additionally, it is evident that there is a pattern of lighter and darker regions on the die surfaces, repeating at approximately 10 degree increments along the die radius. This pattern of coloring is not actually a feature of the surface, but arises from the fact that each set of stitched images (Figs. 10 and 11) were obtained using 27 individual micrographs taken at 10 degree increments (as detailed in Section 2.3). Due to the cylindrical shape of the dies, the surface in the middle of each micrograph is approximately normal to the line of sight of the microscope lens and, therefore, appears brighter. The normal of the surface to the left and right of the centre of the image are at increasing angles from the lens' line of sight and, therefore, appear darker.

#### 3.1.2. Contact region

The horizontal markings along the blank sliding direction and discoloration observed (see Figs. 10 and 11) clearly show that the blank makes sliding contact with the die at the region of approximately 0–75 degrees on the radius surface, during the stamping process. The surfaces outside this region remain unchanged, indicating the areas where sliding contact conditions do not occur. Hence, the region of approximately 0–75 degrees on the die radius is denoted as the 'overall' contact region.

The general wear response prior to failure (Fig. 10) shows two distinct zones within this overall contact region. The region of approximately 0–50 degrees on the die radius shows a darker discoloration and the existence of a larger number of horizontal markings. While the 50–75 degree region shows a reduced number of horizontal markings and less discoloration. This result makes sense, considering the larger sliding distances experienced at approximately the first half of the die radius, as a result of the steady-state stage [14], as shown in Fig. 1b.

The approximate locations of the contact zones – identified by Pereira et al. [13] and shown in Fig. 1 – are indicated at the bottom of Figs. 10 and 11. It is evident that the experimentally observed overall contact region correlates well with the numerically predicted contact zone for the entire stamping process. Furthermore, the two distinct zones observed in Figs. 10 and 11 (described above) correlate well with the steady-state and transient-only contact zones (see Fig. 1).

It is worth noting that the two contact zones are easily visible on the polished dies (dies I–III), at the regions where severe wear is not evident (Fig. 10a–c). However, for the unpolished die (die IV, Fig. 10d), the blank contact zones are not as clear, due to the number and severity of surface defects initially present on the die radius. Additionally, the existence of severe wear and galling (Fig. 11) makes the identification of the two contact zones more difficult. However, in these cases, careful examination does still reveal the existence of the identified overall, steady-state and transient-only contact zones.

The mechanism that causes the discoloration at the die surface is not understood. The discoloration was observed over the die radius and on the flat surfaces of the blank holder and die, clearly indicating the regions where sliding contact with the blank surface has occurred. However, it is surmised that this is a mild mechanism that is not critical to the overall wear response, especially when considering the more severe mechanical wear mechanisms (ploughing, galling) observed, which will be discussed below.

#### 3.1.3. Ploughing mechanism

The sliding and transverse direction *Ra* values, obtained from the profilometry measurements before and after the tests, were examined in an attempt to characterize the wear behavior over the die radius. It was found that the *Ra* parameter did not provide a clear or consistent indication of the location and severity of the wear over the die radii [27]. However, it was found that a comparison of the surface profile deviation over the die radii, calculated before and after the wear tests (Fig. 12), could be used to assess whether material was removed from the die surface during the wear process. Due to the measurement system and location method used, the position of each profile measurement was within approximately ±0.25 mm of the specified value from the die insert edge. Therefore, the two measurements shown in Fig. 12 may not be taken at precisely the same location on the die radius insert surface and cannot be quantitatively compared to each other – i.e. the difference between the two curves cannot be used to calculate the amount of material removed. However, a qualitative comparison of the two curves in Fig. 12 shows that the general shape of the profile is approximately the same for the measurements before and after the test. Therefore, considering the level of correlation between the two curves (with particular reference to the scale of the ordinate in Fig. 12); it is likely that wear mechanisms involving material removal are not dominant. Similar trends were observed for each of the 6 die radii examined in this study.

Close examination of the horizontal markings on the die surfaces, shown in Figs. 10 and 11, reveals that these are comprised

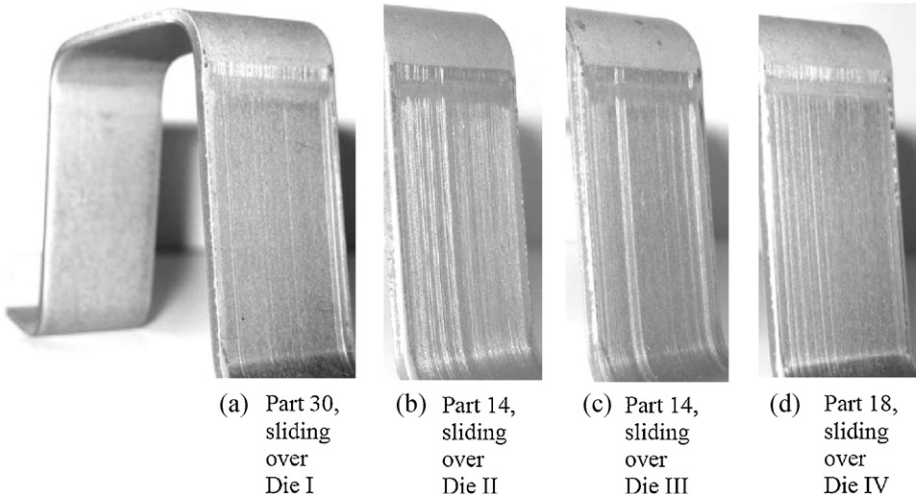


**Fig. 9.** Sidewalls of the last formed parts for Tests I–IV.

of grooves and ridges parallel to the blank sliding direction (see Fig. 13). These visual observations, and the surface profile measurements shown in Fig. 12, indicate that the ploughing asperity deformation mechanism is dominant over much of the die radius surface. This ploughing-type of surface degradation occurs over most of the contact region (i.e. at approximately 0–75 degrees on the die radii), for all die inserts tested. However, Fig. 13 shows that the number of scratches is reduced within the transient-only contact region (at approximately 50–75 degrees on the die radius). This correlates well to the lower sliding distances expected to occur in this region (see Fig. 1b).

### 3.1.4. Galling mechanism

In addition to the ploughing mechanism described above, the galling mechanism is evident on the die radius surface. Galling is the seizure of the sheet surface caused by transfer of the sheet material to the tool surface and it leads to the scratching of the formed sheet surface [18]. Therefore, galling can be identified by observing the

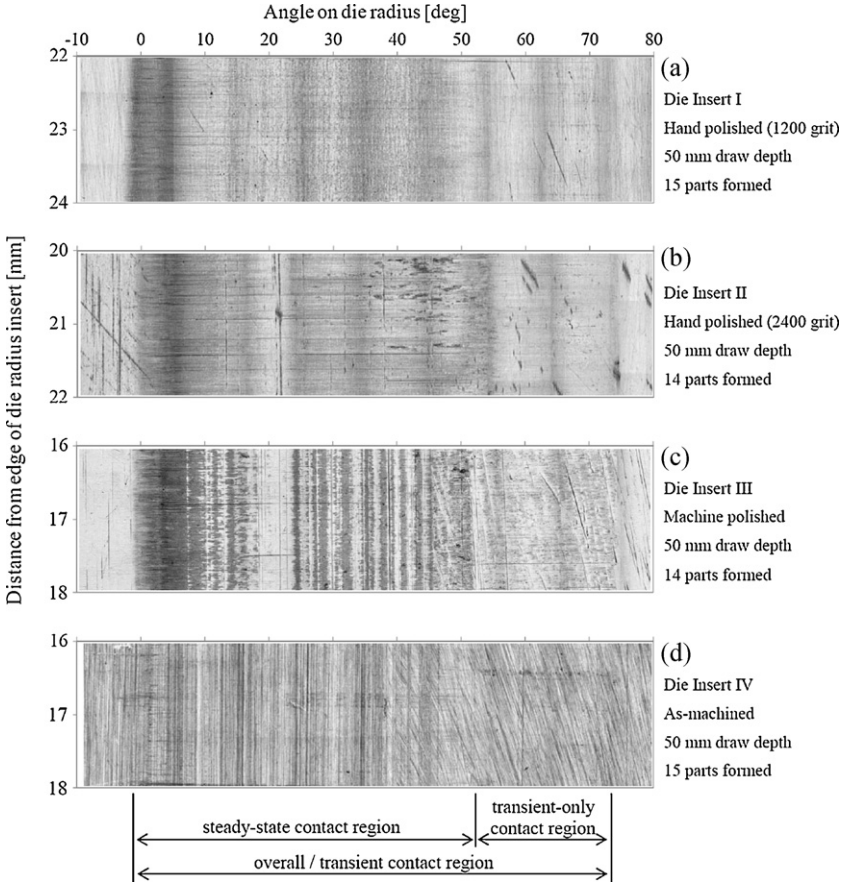


**Fig. 10.** Surfaces of die inserts used for full stroke tests, showing general wear behavior at instances and locations where severe wear (i.e. failure) has not yet occurred. The blank sliding direction is from left to right. The approximate locations of the contact zones, identified by Pereira et al. [13] and shown in Fig. 1, are indicated at the bottom.

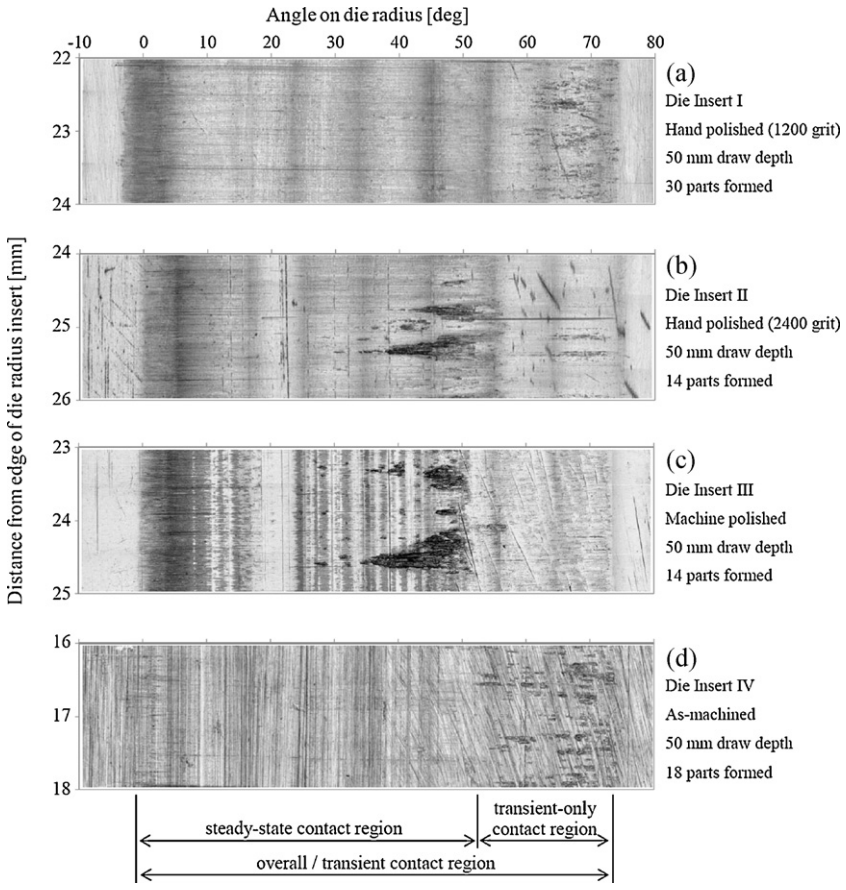


**Fig. 11.** Surfaces of die inserts used for full stroke tests, showing wear behavior at end of tests and at locations where severe wear (i.e. failure) is evident. Blank sliding direction from left to right. The approximate locations of the contact zones, identified by Pereira et al. [13] and shown in Fig. 1, are indicated at the bottom.

surfaces of the die radii and the formed sheet metal. Fig. 11 shows regions on the radii which correspond to the locations of scratches observed on the sidewalls of the stamped channels (refer to Fig. 9). In all cases, failure was caused by severe galling. Therefore, it is clear that the galling mechanism is critical to the overall tool wear response of the stamping process examined.

Initial examination of Fig. 11 shows that the material transferred to the die surface by the galling process occurs at different locations for each of the dies shown. That is, die insert I shows severe galling at approximately 60–75 degrees on the die radius; die II at 35–55 degrees; die III at 25–50 degrees; and die IV at 50–75 degrees on the die surface. However, closer examination of the worn surfaces reveals that, in addition to these regions where localized severe galling is easily visible, small lumps of galling are present over approximately the entire region of 10–75 degrees, for all of the dies tested. For example, Fig. 14 shows evidence of galling over the region of 10–75 degrees on the die radii for both dies I and II. The regions shown in Fig. 14b–f were deliberately chosen to show in detail the same regions visible at a more macro level in Fig. 11a and b. Similar evidence of galling can be found over the same region (10–75 degrees) on dies III and IV.

It is generally understood that galling is a multi-stage process, where the initial stage of local transfer is followed by a stage of growth of the transferred material [18,24,28]. Therefore, from a tool wear analysis perspective, identifying the conditions that cause these initial stages of the galling is of particular importance. The experimental observations indicate that the contact conditions experienced at 10–75 degrees on the die radius are severe enough


**Fig. 12.** Comparison of surface profile deviation of initial surface (0 parts formed) and surface at end of tests (30 parts formed), for die radius I at 20 mm from edge.

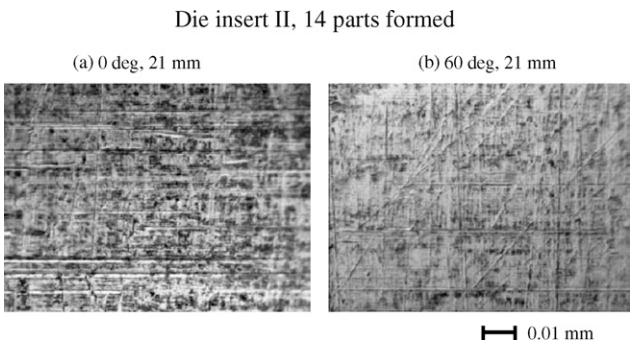


**Fig. 13.** Two locations on the surface of die radius insert II, after 14 parts formed, showing the existence of parallel grooves and ridges in line with sliding direction. Each optical microscope image was taken using a 100× lens, with the approximate angle on the die radius and distance from the edge indicated. The blank sliding direction is from left to right.

to initiate galling. Therefore, it can be concluded that these conditions are critical to the overall tool wear response.

Although it is not of primary importance to the tool wear response, the observation that there are different locations of severe macroscopic galling on each of the dies, can be partly explained by the two-stage nature of the galling process. The growth stage of the galling process, which can be quite rapid, can be influenced by a number of factors, including: contact pressure, shear strength at the interface, asperity angle of attack, asperity height, etc. [24]. This rapid nature of the growth stage is evident by examining the large build up of transferred material that occurred between stamping 15 parts to 18 parts on the surface of die insert IV (see Figs. 10d and 11d). Furthermore, once the growth stage of galling has begun, it is likely to continue at less severe contact conditions, due to the intrinsic adhesion caused by the self contact of the sheet/galled material, and the increased asperity height associated with the built up material.

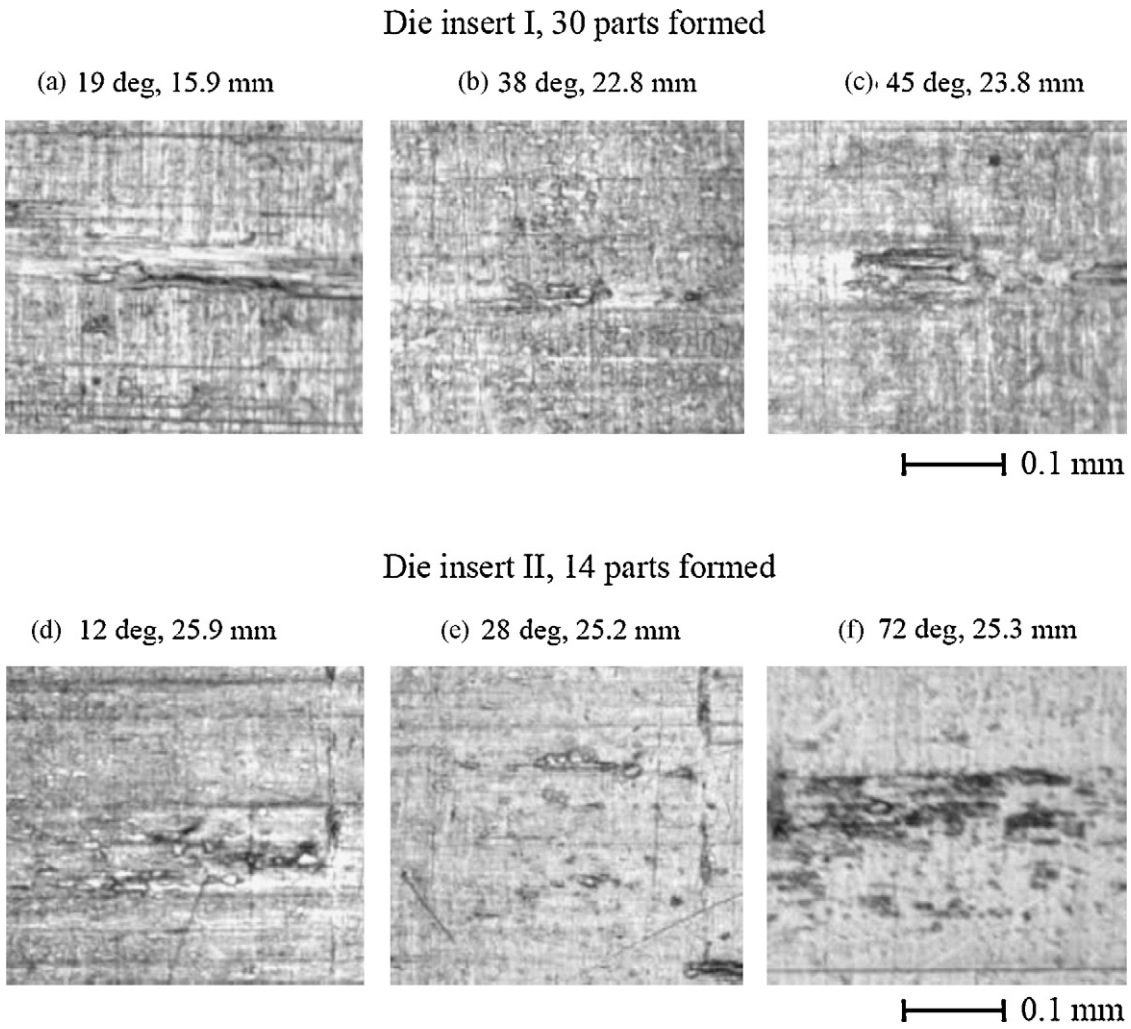


**Fig. 14.** Several locations on the surfaces of die radius inserts I and II, showing the existence of galling over the region of 10–75 degrees on the die radius surface. Each optical microscope image was taken using a 10× lens, with the approximate angle on the die radius and distance from the edge indicated. The blank sliding direction is from left to right.

For both die inserts I and IV, the region of severe macroscopic galling corresponds to the region near the end of the die radius that experiences sliding contact at pressures above 1000 MPa [14]. The increased tendency for further material transfer at lower contact pressures, after galling initiation, can be seen in Figs. 11b and c (die inserts II and III). In these cases, the localized regions of macroscopic galling correspond well with the location of the second contact pressure peak on the die radius that exists during the steady-state stage (see Fig. 1a). Hence, it is likely that after galling was initiated, the large sliding distances and moderate contact pressures that occur during the steady-state stage [14] were sufficient to cause the localized regions of material transfer to grow rapidly. Nonetheless, in all cases, it was evident that galling was initiated at the region of 10–75 degrees on the die radius, with further macroscopic galling growth (and failure) occurring within this region.

The experimental observations show that galling does not occur at the beginning of the die radius (near 0 degrees) for all cases. Therefore, it is evident that the large contact pressures and sliding distances that occur near 0 degrees on the die radius during the steady-state stage of the stamping process (shown in Fig. 1) do not cause galling and are, therefore, not critical to the overall tool wear response. Conversely, it is clear that severe galling occurs in the transient-only contact zone (50–75 degrees on the die radius). Fig. 1a shows that this region of the die surface only contacts the blank during the transient stage of the stamping process. Therefore, any surface degradation observed in this region can only be attributed to the contact conditions that occur during the transient stage (and cannot be associated with the steady-state phase). As such, the wear observations indicate that the transient stage is critical to the overall tool wear response, as will be examined in further detail in Section 3.2.

Finally, the results obtained for Tests I–IV indicate that the different surface preparation methods used for the die insert surfaces did not have a notable effect on the location or type of wear mechanism produced. Due to the stochastic nature of wear testing (and testing in general), the effect of the surface preparation method on the wear rate cannot be determined from the single tests conducted for each condition. However, as will be discussed further in Section 3.3, this was not one of the aims of the study. The primary aim of the study was to characterize the locations of the most severe wear behavior and failure mechanisms over the die radius, such that these could be related to the identified contact conditions. The reason for selecting a variety of surface preparation methods was to ensure that the wear observations obtained were robust and valid for a variety of conditions. It is clear that this aim was achieved, with the overall wear behavior comparing well for each case, thus providing a level of confidence both in the results obtained and the correlation with the numerical predictions observed.

### 3.2. Tool wear response due to transient stage (Tests V and VI)

Based on the characterized overall wear response and knowledge of the contact conditions, a second series of tests were conducted to assess, in isolation, the tool wear response due to the transient stage of the stamping process. Table 3 shows that the test details are the same as that of Test I, except for the shorter drawing depth of 17 mm. This corresponds to the region of punch travel (0–17 mm) necessary to replicate only the transient stage of the stamping process, as shown in Fig. 1a. Hence, the significance of the transient stage on the overall wear response can be clearly shown.

The surface preparation method used in Test I was replicated for Tests V and VI because it produced the most consistent surface topography, largely free from the grinding defects associated with the manufacturing process, and thus was most representative of the surface condition expected on industrial stamping tools. Due to the stochastic nature of wear processes, two tests were conducted to provide a level of confidence in the results obtained.

The surfaces of die inserts V and VI, at locations where failure occurred (i.e. corresponding to regions of light scratches on the stamped parts), are shown in Fig. 15a and b. These regions were chosen to highlight the general wear behavior. Due to the relatively small amount of galled material evident on die insert VI after 13 parts formed (Fig. 15b), Test VI was continued for a further 12 stampings. The same region on die insert VI is shown in Fig. 15b and c, to show the wear progression from 13 to 25 parts formed.

#### 3.2.1. Contact region

Fig. 15 shows that the blank makes sliding contact with the die radius at approximately 0–75 degrees on the die radius. As expected, this is the same as the contact region observed for Tests I–IV, since the transient stage results in the largest angle of contact between the blank and die radius [13] (see Fig. 1a). Additionally, Fig. 15 shows that there is no obvious demarcation within the contact region on the surfaces of die radius inserts V and VI. This result is expected, since the large difference in sliding distances between the steady-state and transient-only contact zones – which caused the demarcation observed on the die radii in Tests I–IV (see Fig. 10) – do not exist in Tests V and VI. Hence, this result correlates well with the contact behavior predicted from the numerical model.

#### 3.2.2. Ploughing mechanism

The ploughing mechanism is evident over the entire contact region of die inserts V and VI, which is comparable to the ploughing behavior observed on die inserts I–IV. The number and severity of the scratches associated with the ploughing mechanism are greater near the start of the contact zone, as compared to near the end, for both dies V and VI. This result compares well with the larger sliding distances that occur at the start of die radius during the transient stage, as illustrated by the numerical sliding distance calculations for the transient stage in isolation [14,27].

It is worth noting that Fig. 15b and c shows a deep groove near 0 degrees on the die radius surface. A small number of these types of grooves were evident near 0 degrees at the end of the tests on all of the die surfaces, as can be seen Figs. 10 and 11. It is speculated that these grooves are caused by the 'pulling out' of carbides near the surface of the die as a result of the ploughing mechanism. Nonetheless, the locations of galling (in terms of the distance from the edge of the die insert), which occur near the end of the die radius, do not correspond to the locations of the deep grooves observed at the beginning of the die radius. Therefore, it can be rationalized that this mechanism is not critical to the overall wear response.

#### 3.2.3. Galling mechanism

As identified in Section 3.1, the galling behavior is critical to the overall tool wear response, as it results in the eventual failure of the stamping process. Close examination of the surfaces shown in Fig. 15 reveals traces of galling on die inserts V and VI at the region of approximately 10–75 degrees on the radius. The fact that galling is similarly distributed over the die radius in the short stroke tests (V and VI), compared to the full stroke tests (I–IV), clearly demonstrates the significance of the identified transient stage of the stamping process on the overall tool wear behavior. Furthermore, the fact that severe wear was observed after a similar number of stamped parts in all tests indicates that the overall tool life is primarily dependent on the severe transient contact conditions.

More galling is evident near 40 degrees on the die radius for die V (Fig. 15a). The reason for this is similar to that described for Tests I–IV. Examination of the contact conditions predicted from the finite element model for the transient stage only shows that a larger amount of sliding occurs, at low contact pressures, near 40 degrees on the die radius [14,27]. However, as previously described,

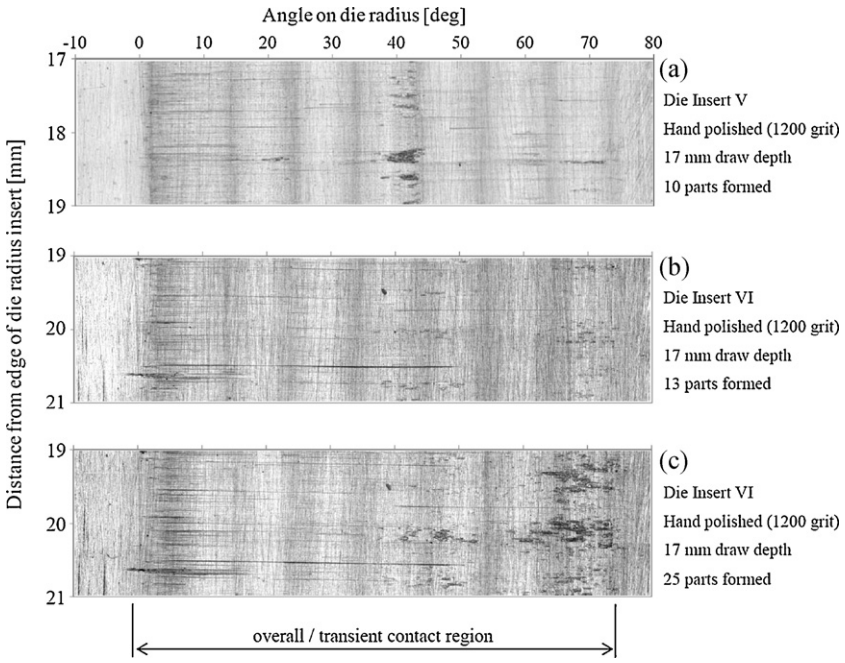


**Fig. 15.** Surfaces of the die inserts used for the short stroke tests, showing the wear contribution of only the transient stage of the stamping process. Blank sliding direction from left to right. The approximate location of the contact zone, identified by Pereira et al. [13] and shown in Fig. 1, is indicated at the bottom.

once galling is initiated, these lower contact pressure conditions are sufficient to cause the localized regions of material transfer to grow rapidly, resulting in severe macroscopic galling.

### 3.3. Final remarks on wear at the die radius

It is clear that the stamping process examined in this study results in a system that is highly prone to wear and galling. Consequently, degradation of the die radius surface was observed after only a small number of stamping operations. It was known prior to conducting the tests that the combination of: a relatively small die radius, the use of advanced high strength steel sheet sliding against an uncoated tool steel surface, and the fact that lubricant was not used, would represent a tribologically severe process. These experimental settings were chosen deliberately, due to the time-consuming nature of the laboratory-based channel forming wear test.

The authors are aware that reducing the time scale of wear tests, to speed up the production of data, can have the danger of moving from a regime of operation where one wear mechanism is dominant to another regime controlled by different surface degradation mechanisms [29]. However, it is known that galling is a common failure mode for sheet metal stamping dies [17,22,29]. It is clear that this wear mechanism was represented in the channel forming wear tests conducted in this investigation. Additionally, previous studies have shown that lubrication has little effect on the occurrence of the severe mechanical wear modes of galling, wedge forming and ploughing [18,30].

The use of accurate loading conditions is particularly important when the aim of the test is to obtain wear rates for a given material combination and process conditions, for subsequent use in wear models or estimating wear life. The aim of the channel forming tests presented in this paper, however, was to primarily characterize the locations of the most severe wear over the die radius, such that these could be related to the identified contact conditions. The exact wear rate achieved was not of importance and was not studied.

For these reasons, it is clear that the existence of these severe tribological conditions does not detract from the originality and significance of the results presented and the conclusions drawn. To the authors' knowledge, the precise locations and types of wear mechanism over the die radius for a sheet metal stamping process have not been previously reported in the literature. Furthermore, this is the first time that the overall tool wear response and tool life has been shown to be primarily dependent on the transient contact and deformation conditions experienced at the die radius and blank surfaces. The results have shown that the severe contact pressure/small sliding distance conditions found to occur during the initial portion of the stamping process are critically important to the overall wear behavior.

It has been shown that the severe contact conditions are due to the specific bulk deformation conditions that occur at the blank surface as it is initially formed over the die radius [15]. It is likely that the combination of deformation conditions and severe contact stresses that occur during the transient stage, which is critical to the overall wear response, are not accurately captured by traditional wear tests and micromechanical wear models. Hence, the applicability of traditional wear tests and models for use in the sheet metal stamping industry may be questionable. Therefore, the findings from this work may assist future research on the development and application of suitable wear tests, which correctly replicate the important contact and deformation conditions that occur during real stamping processes.

## 4. Summary

In this paper, a new laboratory-based channel forming test and analysis procedure was detailed, in order to study tool wear in sheet metal stamping. The locations of specific wear mechanisms over the die radius, and their relative severity, have been detailed for a typical sheet metal stamping process. Importantly, the wear behavior observed was not one of pure material removal, and therefore replicated the type of wear response commonly observed on hardened industrial stamping tools.

It was shown that the wear over the die radius primarily consisted of a combination of ploughing and galling mechanisms. The ploughing mechanism was found to occur over the entire blank contact region, with two distinct zones observed within the overall

contact region. The location of these zones, and the relative severity of the wear observed, were shown to correlate well with the steady-state and transient-only contact regions reported in previous finite element studies. The galling wear mechanism, observed over most of the die radius surface, was found to result in failure of the sheet metal stamping process and is, therefore, critical to the overall tool wear response. Notably, the galling mechanism was not observed near the beginning of the die radius – i.e. the region which experiences the large sliding distances and moderate contact pressures associated with the steady-state stage of the stamping process.

A second series of channel forming tests were conducted in order to assess the importance of the identified transient stage on the overall wear behavior. The galling behavior, which was previously found to be critical to the overall wear response, was found to primarily occur during the transient stage of the process. This result clearly demonstrated that the overall tool wear response and tool life for the channel forming process is primarily dependent on the transient contact and deformation conditions experienced at the die radius and blank surfaces. This is the first time that the severe contact pressure/small sliding distance conditions, which occur during the initial portion of the stamping process, have been shown to be critically important to the overall tool wear response. These findings have direct implications with regards to the applicability of traditional wear tests and models for use in the sheet metal stamping industry.

## Acknowledgements

This research was supported by Ford Motor Company USA, Ford of Australia, Volvo Cars Sweden, and an Australian Research Council Linkage Project (LP0776913). The authors extend their gratitude to Professor Peter Hodgson from Deakin University for his support.

## References

[1] Ö.N. Cora, M. Koç, Experimental investigations on wear resistance characteristics of alternative die materials for stamping of advanced high-strength steels (AHSS), International Journal of Machine Tools and Manufacture 49 (2009) 897–905.
[2] A. Gåård, P. Krakhmalev, J. Bergström, Wear mechanisms in deep drawing of carbon steel – correlation to laboratory testing, Tribotest 14 (2008) 1–9.
[3] E. van der Heide, A.J. Huis in t Veld, D.J. Schipper, The effect of lubricant selection on galling in a model wear test, Wear 251 (2001) 973–979.
[4] C. Boher, D. Attaf, L. Penazzi, C. Levaillant, Wear behaviour on the radius portion of a die in deep-drawing: identification, localisation and evolution of the surface damage, Wear 259 (2005) 1097–1108.
[5] S. Christiansen, L. De Chiffre, Topographic characterization of progressive wear on deep drawing dies, Tribology Transactions 40 (1997) 346–352.
[6] M. Eriksen, The influence of die geometry on tool wear in deep drawing, Wear 207 (1997) 10–15.
[7] P. Groche, G. Nitzsche, A. Elsen, Adhesive wear in deep drawing of aluminum sheets, CIRP Annals – Manufacturing Technology 57 (2008) 295–298.
[8] D. Hortig, D. Schmoeckel, Analysis of local loads on the draw die profile with regard to wear using the FEM and experimental investigations, Journal of Materials Processing Technology 115 (2001) 153–158.
[9] J. Mortensen, J. Dirks, P. Christensen, A combined physical and numerical simulation of tool performance in conventional deep-drawing operations, in: Proc. IDDRG 18th Biennial Congress, Lisbon, Portugal, 1994, pp. 233–240.
[10] D. Casellas, I. Picas, A. Llobet, R. Hernández, M. Riera, I. Valls, B. Casas, Mechanical performance of tools in cold forming of high-strength steels, in: Proc. International Conference on New Developments in Advanced High-Strength Sheet Steels, Orlando, USA, 2008, pp. 391–400.
[11] M.R. Jensen, F.F. Damborg, K.B. Nielsen, J. Danckert, Applying the finite-element method for determination of tool wear in conventional deep-drawing, Journal of Materials Processing Technology 83 (1998) 98–105.
[12] A. Thuvander, O. Sandberg, Computation of die loads in sheet forming using dies of tool steel with improved anti-galling properties, in: Proc. International Symposium on Friction, Wear and Wear Protection 2008, Aachen, Germany, 2008, pp. 333–338.
[13] M.P. Pereira, W. Yan, B.F. Rolfe, Contact pressure evolution and its relation to wear in sheet metal forming, Wear 265 (2008) 1687–1699.
[14] M.P. Pereira, W. Yan, B.F. Rolfe, Sliding distance, contact pressure and wear in sheet metal stamping, Wear 268 (2010) 1275–1284.
[15] M.P. Pereira, J.L. Duncan, W. Yan, B.F. Rolfe, Contact pressure evolution at the die radius in sheet metal stamping, Journal of Materials Processing Technology 209 (2009) 3532–3541.
[16] H. Hoffmann, G. Nürnberg, K. Ersoy-Nürnberg, G. Herrmann, A new approach to determine the wear coefficient for wear prediction of sheet metal forming tools, Production Engineering 1 (2007) 357–363.
[17] O. Sandberg, P.-Å. Bustad, B. Carlsson, M. Fällström, T. Johansson, Characterisation of tool wear in stamping of EHS and UHS steel sheets, in: Proc. International Conference on Recent Advances in Manufacture & Use of Tools & Dies and Stamping of Steel Sheets, Olofström, Sweden, 2004, pp. 151–170.
[18] E. Schedin, B. Lehtinen, Galling mechanisms in lubricated systems: a study of sheet metal forming, Wear 170 (1993) 119–130.
[19] G.J. Coubrough, M.J. Alinger, C.J. Van Tyne, Angle of contact between sheet and die during stretch-bend deformation as determined on the bending-under-tension friction test system, Journal of Materials Processing Technology 130–131 (2002) 69–75.
[20] K. Hanaki, K. Kato, Pressure peak in bending and unbending process, Advanced Technology of Plasticity 1 (1984) 581–586.
[21] K. Ersoy-Nürnberg, G. Nürnberg, M. Golle, H. Hoffmann, Simulation of wear on sheet metal forming tools – an energy approach, Wear 265 (2008) 1801–1807.
[22] M. Liljengren, K. Kjellsson, D. Wiklund, Guidelines for die materials, hardening methods and surface coatings for forming of high, extra high and ultra high strength steel sheets (HSS/EHSS/UHSS), in: Proc. IDDRG 2008 Conference, Olofström, Sweden, 2008, pp. 603–614.
[23] T. Skåre, F. Krantz, Wear and frictional behaviour of high strength steel in stamping monitored by acoustic emission technique, Wear 255 (2003) 1471–1479.
[24] M.B. de Rooij, D.J. Schipper, Analysis of material transfer from a soft workpiece to a hard tool: Part I – Lump growth model, Journal of Tribology 123 (2001) 469–473.
[25] Taylor Hobson Limited, Exploring Surface Texture: A Fundamental Guide to the Measurement of Surface Finish, Taylor Hobson Ltd., Leicester, England, 2003.
[26] ISO 4288: 1996, Geometrical Product Specifications (GPS) – Surface Texture: Profile Method – Rules and Procedures for the Assessment of Surface Texture, International Organization for Standardization, 1996.
[27] M.P. Pereira, Tool wear analysis in sheet metal stamping, PhD Thesis, Deakin University, Geelong, Australia, 2009.
[28] A. Gåård, P. Krakhmalev, J. Bergström, Wear mechanisms in galling: cold work tool materials sliding against high-strength carbon steel sheets, Tribology Letters 33 (2009) 45–53.
[29] J.A. Williams, Wear modelling: analytical, computational and mapping: a continuum mechanics approach, Wear 225–229 (1999) 1–17.
[30] K. Kato, T. Kayaba, Y. Endo, Three dimensional shape effect on abrasive wear, Journal of Tribology 108 (1986) 346–351.